Structural rearrangements between portal protein subunits are essential for viral DNA translocation

Ana Cuervo, Marie-Christine Vaney, Alfred A. Antson, Paulo Tavares, Leonor Oliveira

THE JOURNAL OF BIOLOGICAL CHEMISTRY VOL. 282, NO. 26, pp. 18907–18913, June 29, 2007

Structural Rearrangements between Portal Protein Subunits Are Essential for Viral DNA Translocation*

Received for publication, March 1, 2007, and in revised form, April 9, 2007 Published, JBC Papers in Press, April 18, 2007, DOI 10.1074/jbc.M701808200

Ana Cuervo[‡1], Marie-Christine Vaney[‡2], Alfred A. Antson[§], Paulo Tavares[‡3], and Leonor Oliveira[‡4]

From the [‡]Unité de Virologie Moléculaire et Structurale, Unité Mixte de Recherche (UMR) CNRS 2472, UMR Institut National de la Recherche Agronomique (INRA) 1157 and Institut Fédératif de Recherche 115, Bat. 14B, Avenue de la Terrasse, 91198 Gif-sur-Yvette Cedex, France and the [§]York Structural Biology Laboratory, Department of Chemistry, University of York, York Y010 5YW, United Kingdom

Transport of DNA into preformed procapsids is a general strategy for genome packing inside virus particles. In most viruses, this task is accomplished by a complex of the viral packaging ATPase with the portal protein assembled at a specialized vertex of the procapsid. Such molecular motor translocates DNA through the central tunnel of the portal protein. A central question to understand this mechanism is whether the portal is a mere conduit for DNA or whether it participates actively on DNA translocation. The most constricted part of the bacteriophage SPP1 portal tunnel is formed by twelve loops, each contributed from one individual subunit. The position of each loop is stabilized by interactions with helix α-5, which extends into the portal putative ATPase docking interface. Here, we have engineered intersubunit disulfide bridges between α-5s of adjacent portal ring subunits. Such covalent constraint blocked DNA packaging, whereas reduction of the disulfide bridges restored normal packaging activity. DNA exit through the portal in SPP1 virions was unaffected. The data demonstrate that mobility between α-5 helices is essential for the mechanism of viral DNA translocation. We propose that the α-5 structural rearrangements serve to coordinate ATPase activity with the positions of portal tunnel loops relative to the DNA double helix.

Portal proteins are hollow oligomers localized asymmetrically at a single vertex of icosahedral capsids of tailed bacteriophages and herpesviruses (1, 2) providing a tunnel for double-stranded DNA entry and exit (see Fig. 1, *A–C*) (5–7). The viral genome is packaged into procapsids by a DNA translocation motor that assembles at the portal vertex of the procapsid structure (step from states I to II of Fig. 1*A*). The motor is composed of the portal protein, an ATPase (large terminase subunit), and a third component (small terminase subunit or a pRNA) (8). How this large complex uses ATP hydrolysis (9–13) to pump double-stranded DNA against a steep concentration gradient remains a mystery. Although it is well established that the ATPase energetically fuels DNA translocation, biochemical and genetic evidence shows also that the portal protein regulates ATPase activity (13) and that portal mutations impair DNA packaging (13–16). However, a mechanistic role of the portal protein and the function of its cross-talk with the terminase in the DNA packaging reaction remain to be demonstrated. X-ray structures of portal proteins from bacteriophages phi29 (p10) (5) and SPP1 (gp6) (17) show that they share a very similar structure. Their most unusual feature is the presence of a prominent distortion in helix α6. Helix α6 of the SPP1 portal presents a 136° kink stabilized by hydrogen bonding with crown residues and by van der Waals interactions with the carboxyl terminus of helix α5 (see Fig. 1*C*) (17). In isolated gp6, a 13-mer, helices α5 and α6 are connected by a loop that protrudes to the portal tunnel interior (17). This region is disorganized in the phi29 portal structure (5).

The gp6 form found in viral procapsids is a 12-mer. Because no crystallographic structure is available for this oligomeric state, single subunits of gp6 were fitted into the cryoelectron microscopy reconstruction of the portal 12-mer present in viral particles (18) to produce a pseudoatomic model of the gp6 dodecamer (17). The model, which fits well the electron microscopy maps, shows that the portal oligomer maintains architectural features similar to the 13-mer, except for the crown and tunnel loops that undergo positional changes (17). These loops define the most constricted region of the tunnel (see Fig. 1*C*) (17). Its ~18-Å diameter found in the viral particle portal implies that tunnel loops must change their position during viral genome passage to avoid clashing with DNA phosphate groups (see Fig. 1*C*). Inspection of the structure reveals a likely conformational change, and large shifts in the loop positions could be permitted by straightening of the kinked helix α6, concomitant with small displacements of α5-disrupting van der Waals interactions between these two structural elements that stabilize the α6 kink (see Fig. 1*C*) (17). Helix α5 is the component of this molecular lever that connects tunnel loops to the putative binding site of the viral ATPase (see Fig. 1*C*). To address experimentally the hypothesis that positional adjustments between α5 of adjacent subunits are required for the mechanism of viral DNA translocation, we characterized DNA traffic through a portal oligomer reversibly cross-linked

* This work was funded by a Wellcome Trust fellowship (to A. A. A.) and Action Thématique et Incitative sur Programme from the CNRS (to P. T.). The costs of publication of this article were defrayed in part by the payment of page charges. This article must therefore be hereby marked "*advertisement*" in accordance with 18 U.S.C. Section 1734 solely to indicate this fact.

[1] Recipient of a doctoral fellowship from Ministère de l'Education Nationale, de la Recherche et de la Technologie (France).

[2] Present address: Unité de Virologie Structurale and Unité de Recherche Associée 3015 CNRS Département de Virologie, Institut Pasteur, 25 rue du Dr. Roux, 75724 Paris Cedex 15, France.

[3] To whom correspondence should be addressed: Unité de Virologie Moléculaire et Structurale, UMR CNRS 2472 and UMR INRA 1157, Bat. 14B, Ave. de la Terrasse, 91198 Gif-sur-Yvette Cedex, France. Tel.: 33-169823860; Fax: 33-169824308; E-mail: tavares@vms.cnrs-gif.fr.

[4] Supported by post-doctoral fellowships from European Molecular Biology Organization, Fundação para a Ciência e Tecnologia (Portugal), and CNRS.

through the α5 helices. The results show that DNA packaging requires motions of these helices, demonstrating for the first time the mechanistic role of the portal in the process.

EXPERIMENTAL PROCEDURES

Molecular Modeling—The double cysteine gp6 mutants were predicted to form intersubunit disulfide bridges by molecular modeling using the x-ray structure of the isolated $gp6_{SizA}$ 13-mer (Protein Data Bank accession code 2JES (17)) and the pseudoatomic model of the gp6 12-mer. The model was built by fitting gp6 subunits into the cryoelectron microscopy maps of the gp6 12-mer present in the SPP1 structure (EBI accession code EMD-1021 (18)) as described by Lebedev *et al.* (17). Disulfide bonds were designed using reported geometrical parameters from different analyses (Ref. 19 and references therein). Molecular modeling was performed using the Quanta (Accelrys) and Coot programs (20).

Bacteriophages, Bacterial Strains, Plasmids, and Mutagenesis—SPP1 suppressor-sensitive mutant phages SPP1*sus115* (defective in portal protein gp6 production (21)) and *sus70sus115* (defective in production of the terminase small subunit gp1 and of gp6 (15)), SPP1*sizA* (which leads to a 2.7-kbp undersizing of the SPP1-packaged genome (21)), and SPP1*delX* (which carries a deletion in the SPP1 genome dispensable region (21)) were described previously (15, 21). SPP1*sus115delX* was obtained by mixed infection of *Bacillus subtilis* HA101B with SPP1*sus*115 and SPP1*delX* at an input multiplicity of 10 phages/bacterium. The presence of mutation *sus115* in the progeny was assayed by replica spotting in permissive and non-permissive strains, whereas *delX* was identified by the absence of signal in phage spots after DNA-DNA hybridization with a probe specific for the genome region deleted in this phage. Virions carrying different portal proteins were produced by SPP1*sus115delX* infection of *B. subtilis* strains bearing a plasmid that codes for the desired gp6 version (16). The presence of deletion *delX* in the phage genome is necessary to obtain infectious progeny phages, because the *sizA* mutation, present in all gene *6* alleles studied in this work (see below), leads to undersizing of SPP1-packaged DNA molecules. Deletion of a non-essential region allows encapsidation of the complete set of SPP1-essential genes in the presence of *sizA*, enabling viability of the progeny (21). *B. subtilis* HA101B (*sup-3*) and YB886 (*sup*^{o}) were the permissive and non-permissive strains used for SPP1 multiplication (22). The *Escherichia coli* strain used for site-directed mutagenesis was XL-1 Blue (Stratagene). The plasmid vector used in all of the genetic manipulations is a derivative of vector pHP13 carrying the inducible promoter $P_{N25/0}$ (pPT100) as described in Ref. 15.

Gene *6* bearing mutation C55S was engineered by site-directed mutagenesis using the Kunkel method (23) in a template spanning the complete gene *6*. This HpaI-SalI fragment (coordinates 2267–3917 of the SPP1 nucleotide sequence; GenBank™ accession number X97918) was transferred into the SmaI-SalI sites of pPT100, generating plasmid pAC1. In a second step, a fragment Asp-^{718}-PstI carrying mutation N365K from plasmid pSPWA (21) was subcloned into pAC1 cleaved with the same enzymes, generating pAC2. The gene *6* alleles coding for the gp6 single and double cysteine mutants were engineered by site-directed mutagenesis using the QuikChange site-Directed mutagenesis kit (Stratagene) with pAC2 as the template. Complete sequencing of gene *6* alleles was carried out at the central facility of the Centre de Génétique Moléculaire (Gif-sur-Yvette, France). Plasmids carrying the correct gene *6* alleles were purified using a Qiagen kit. Inducible expression from the $P_{N25/0}$ promoter was controlled by the LacI repressor coded by plasmid pGB3 in *E. coli* XL1-blue and pEB104 in *B. subtilis* YB886 (15).

Assay for Disulfide Bridge Formation in gp6—Disulfide bridge formation in gp6 proteins carrying mutations to single or double cysteines was tested for the gp6-isolated form in *B. subtilis* extracts (16) and for gp6 assembled either in SPP1-purified procapsids (24) or CsCl-purified phages. *B. subtilis* crude extracts (~70 μg total protein) or procapsids (25 nM) were incubated in the presence or in the absence of 4 mM dithiothreitol (DTT)[5] for 1 h at 37 °C. Samples were treated with 10 mM *N*-ethylmaleimide for 1 h at 37 °C to alkylate free sulfhydryl groups. Phages (~5×10^9 infective phages) were treated with 4 mM DTT, disrupted with 50 mM EDTA, followed by incubation with 10 units of benzonase in the presence of 100 mM $MgCl_2$, as described previously (25). Samples were mixed with SDS-PAGE loading dye lacking reducing agents, boiled for 5 min, and resolved in 12% SDS-polyacrylamide gels. After immunoblotting, gp6 was detected using an anti-gp6 polyclonal serum and the ECL detection system (Amersham Biosciences). Purified gp6 cross-linked with glutaraldehyde (27) was used as the control for migration in SDS-PAGE of covalently linked gp6 13-mers.

DNA Packaging in Vitro—Procapsids containing different gp6 forms were produced by *trans*-complementation *in vivo* and purified as described previously (13). DNA packaging reactions were carried out using the SPP1 *in vitro* DNA packaging system with purified components (24). Before setting up the packaging reactions, procapsids (15 nM) were incubated in the presence or in the absence of 2 mM DTT for 1 h at 37 °C.

DNA Ejection in Vitro—Phage particles (~10^9 infective particles/lane in Fig. 4) were pretreated with 10 μg/ml DNase and 0.5 mg/ml RNase at 37 °C for 1 h in ejection buffer (100 mM Tris-HCl, pH 7.5, 300 mM NaCl, and 10 mM $MgCl_2$). The samples were then split and reduced with 2 mM DTT or left untreated for 15 min at 37 °C. After cooling down for 15 min on ice, the SPP1 receptor ectodomain was added to a stoichiometry of 2000 YueB780 dimers (26) per viable phage. After 15 min on ice, the samples were shifted to 15 °C to trigger DNA ejection. Reactions were stopped and then deproteinized, and DNA protected from DNase was resolved by pulsed field gel electrophoresis as described previously (25).

RESULTS AND DISCUSSION

Engineering of Intersubunit Disulfide Bridges in SPP1 Portal Oligomers—To check whether α5–α5 motions are required for DNA packaging, we engineered disulfide bridges to immobilize reversibly these helices (Fig. 1, *D* and *E*). To avoid undesired covalent links between one cysteine residue present in the wild-type SPP1 portal protein (Cys^{55}) and the single or double cysteine mutants to be engineered, the Cys^{55} residue was replaced by a serine. $Gp6_{C55S}$ was fully functional (data not shown). A

[5] The abbreviation used is: DTT, dithiothreitol.

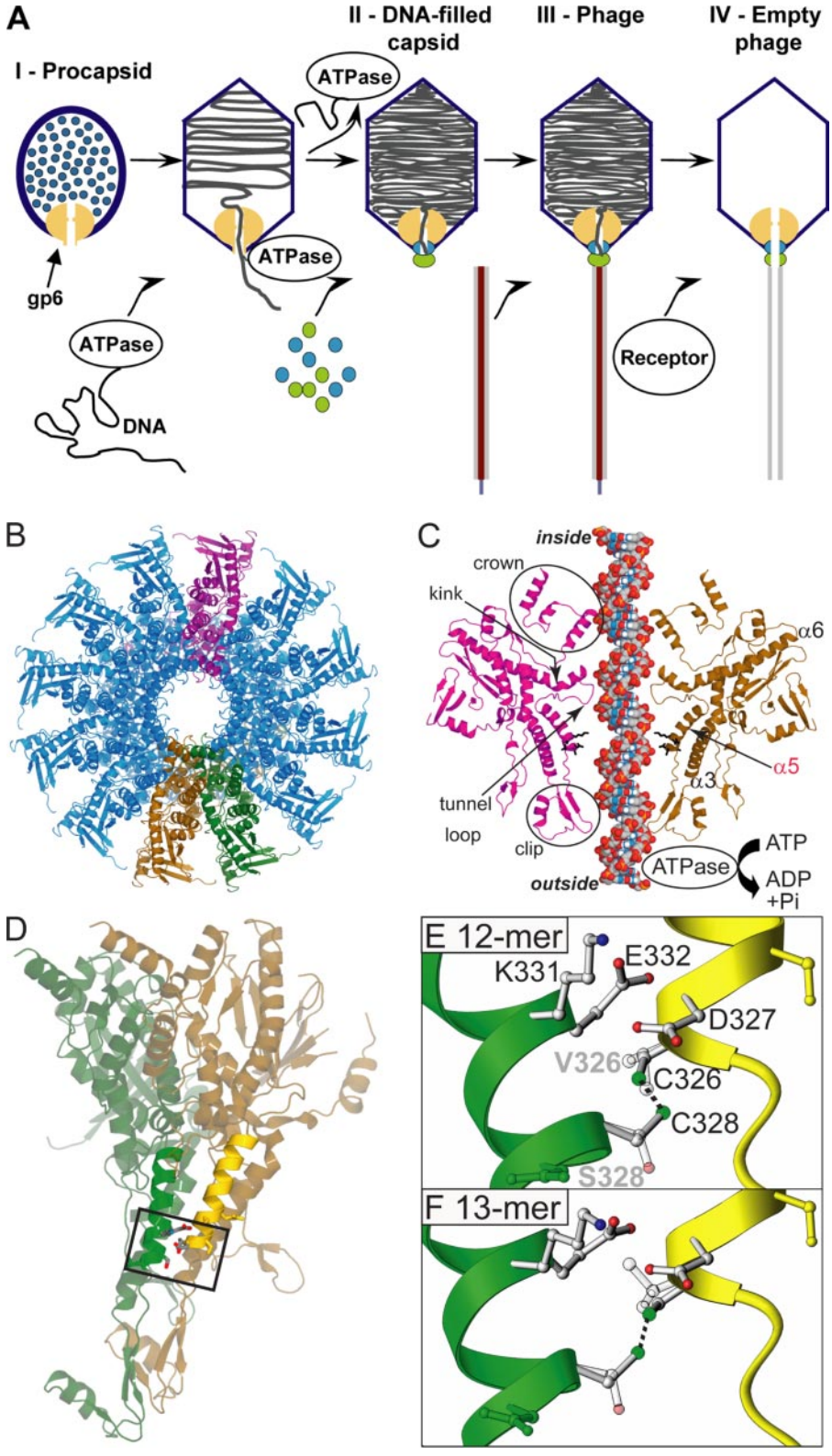

FIGURE 1. **Structure of the bacteriophage SPP1 portal protein and modeling of intersubunit disulfide bridges.** *A*, schematic representation of SPP1 morphogenetic steps. The portal protein gp6 is represented in *yellow*. The head completion proteins gp15 and gp16 are represented in *blue* and *green*, respectively. *B*, ribbon diagram of the portal protein 12-mer viewed along the tunnel axis from the interior of the phage capsid. Two adjacent subunits are *highlighted* in *brown* and *green*. The subunit symmetric to the one in *brown* is shown in *purple*. *C*, ribbon diagram of two symmetric subunits (color-coded as in *B*) with the B-form DNA (van der Waals model) fitted inside the tunnel. Gp6 mutations studied in this work are rendered in *black*. Structural elements of gp6 and the putative interface of interaction with the viral ATPase are indicated. *D*, ribbon diagram of two adjacent gp6 subunits viewed from inside the portal tunnel. Side chains of the five residues in helix α5 that were mutated to create double cysteine mutants (D327C/S328C, V326C/S328C, V326C/K331C, and V326C/E332C) are represented in *ball* and *stick* format. *E* and *F*, enlargements of the rectangle in *D* (gp6 12-mer) and of the same region of the gp6 13-mer, respectively, showing modeled cysteines that form the disulfide bridge C326–C328 (*dashed line*). The original residues found on the gp6 structure were rendered semi-transparent. Structures are presented using PyMOL (*B*, *C*, and *D*) (Delano Scientific LLC, San Francisco, CA) and RIBBONS (*E* and *F*) (4).

TABLE 1

Modeling of disulfide bridges in the SPP1 portal protein

Distances between the Cα atoms are from the 13-mer and 12-mer gp6 structures (17). Distances between the sulfur atoms and bond angles correspond to modeled cysteine side chains. Geometrical parameters for disulfide bridges (*) are from Ref. 19. ND, not done.

Mutant	Structure	Distance Cα–C′α	Distance Sγ–S′γ	Angle C$_\beta$–Sγ-S′γ	Angle C′$_\beta$-S′γ-Sγ	Dihedral Angle C$_\beta$-Sγ-S′γ-C$_\beta$′
		Å	*Å*	*degrees*	*degrees*	*degrees*
Ideal values*		5.4 (RH), 5.8 (LH)	2.02	105	105	−80 (LH), +100 (RH)
D327C/S328C	13-mer (X-tal)	7.3	4.8	ND	ND	ND
V326C/S328C	13-mer (X-tal)	6.0	2.0	104.8	128.7	−89.3
V326C/K331C	13-mer (X-tal)	7.2	2.1	133.2	144.3	−86.2
V326C/E332C	13-mer (X-tal)	6.4	1.9	133.8	130.1	−110.1
D327C/S328C	12-mer (model)	6.2	2.1	153.3	135.3	−126.8
V326C/S328C	12-mer (model)	6.6	2.0	143.5	129.9	−134.4
V326C/K331C	12-mer (model)	7.8	3.7	ND	ND	ND
V326C/E332C	12-mer (model)	5.6	2.1	103.0	85.8	−89.4

TABLE 2

Characterization of simple and double gp6 cysteine mutants

ND, not done.

Cysteine mutants[a]	Titre[b]	gp6 production[c]	gp6 incorporation in procapsids[d]	S-S cross-linking of gp6 (13-mer)[e]	S-S cross-linking of gp6 in procapsids (12-mer)[e]
	% control				
Control	100	+++	+++	No	No
V326C	49 ± 6 (3)	+++	+++	Dimer	Dimer
D327C	ND	ND	ND	ND	ND
S328C	27 ± 6 (4)	+++	+++	Dimer	Dimer
K331C	23 ± 8 (3)	+++	ND	Dimer	ND
E332C	60 ± 3 (3)	+++	ND	Dimer	No
D327C/S328C	5 (1)	+++	++	Multimer	Multimer
V326C/S328C	84 ± 2 (4)	+++	+++	Multimer	Multimer
V326C/K331C	14 ± 9 (3)	+++	+	Multimer	No
V326C/E332C	14 ± 4 (3)	+++	+	Multimer	Multimer

[a] Mutant gp6 forms characterized in this work. Control gp6, parental of all proteins studied here, carries mutations C55S and N365K.

[b] Severity of the amino acid substitutions in portal protein function quantified by complementation assays *in vivo* (16). Results are expressed as the percentage of control gp6. The numbers within parentheses indicate the number of independent experiments carried out.

[c] gp6 accumulation in extracts of *B. subtilis* YB886 (pEB104) strains bearing a plasmid coding for the different gp6 mutant proteins. The relative intensity of the gp6 signal in Western blot was expressed by comparison to the amount detected for control gp6.

[d] gp6 incorporation in procapsids. Samples of purified procapsids were normalized according to the levels of gp13 present in each procapsid preparation, as estimated from Coomassie Blue-stained gels (see Fig. 2*A*). gp6 was detected by Western blot (see Fig. 2*B*). The relative intensity of the gp6 signal in Western blot was expressed by comparison to the amount detected for control gp6.

[e] Disulfide bridge formation assayed by electrophoresis of reduced (treated with 4 mM DTT) and non-reduced samples, treated with 10 mM *N*-ethylmaleimide before denaturation in a non-reducing SDS buffer. Extracts of *B. subtilis* cells and purified procapsids containing the gp6 mutant proteins were used as the source of gp6 13- and 12-mer forms, respectively. gp6 was detected by Western blot. gp6 covalently bound dimers and multimers correspond to the bands gp6$_2$ and gp6$_{HMW}$ in Fig. 2*C*, respectively.

gp6 protein containing both the C55S and N365K (gp6$_{SizA}$) substitutions was then generated. This was justified by the presence of substitution N365K in the available crystallographic structure of gp6 (17). Hereinafter the gp6$_{C55S\ N365K}$ protein will be designated as control gp6.

The close distance between α5 of neighbor subunits allowed designing mutations to cysteine residues whose distance and geometry are compatible with disulfide bridge formation (Table 1). Modeling was carried out both for the atomic structure of the isolated gp6 13-mer and for the pseudoatomic structure of the gp6 12-mer purified from viral particles (17). Five residues (Val^{326}, Asp^{327}, Ser^{328}, Lys^{331}, and Glu^{332}) were predicted to establish different types of intersubunit disulfide bonds in the 13-mer (V326C/S328C, V326C/K331C, and V326C/E332C) and in the 12-mer (V326C/S328C, V326C/E332C, and D327C/S328C) (Fig. 1, *E* and *F*, and Table 1). Note that substitutions V326C/K331C and D327C/S328C are anticipated to form disulfide bonds exclusively in the 13-mer and 12-mer, respectively, due to structural differences between the two oligomeric states. Single and double mutations into cysteine were next introduced in the control gp6 coding gene by site-directed mutagenesis. All mutant proteins were produced to normal amounts in *B. subtilis*, the bacterial host of bacteriophage SPP1 (Table 2).

Intersubunit disulfide bond formation *in vitro* was checked in cell extracts containing gp6 13-mers or purified procapsids carrying gp6 12-mers by SDS-PAGE under non-reducing conditions. Purified gp6 cross-linked with 25 mM glutaraldehyde was used as the control for electrophoretic mobility of covalently bound gp6 oligomers (27). Air oxidation was sufficient for the formation of disulfide bridges. Oxidant agents such as 55′-dithiobis-2-nitrobenzoic acid or diamide did not cause a significant improvement in the reaction (data not shown). Single substitutions to cysteine led to the formation of some covalently bound dimers of gp6 subunits in a non-reducing environment (Fig. 2*C* and Table 2). These dimers are not an artifact due to disulfide bridge formation during sample preparation, because their presence is not eliminated by alkylation of free thiol groups with *N*-ethylmaleimide prior to denaturation of samples for SDS-PAGE. Formation of structurally unexpected disulfide bridges in a protein population was previously reported for other multimeric proteins (28). Double mutants formed gp6 high molecular weight complexes (gp6$_{HMW}$), similar to those of purified gp6 after glutaraldehyde cross-linking (Fig. 2*C*). Gp6$_{HMW}$ disappeared when proteins were incubated with the reducing agent DTT, indicating that disulfide bond formation in an oxidizing environment was successfully achieved (Fig. 2*C* and data not shown). The resolution

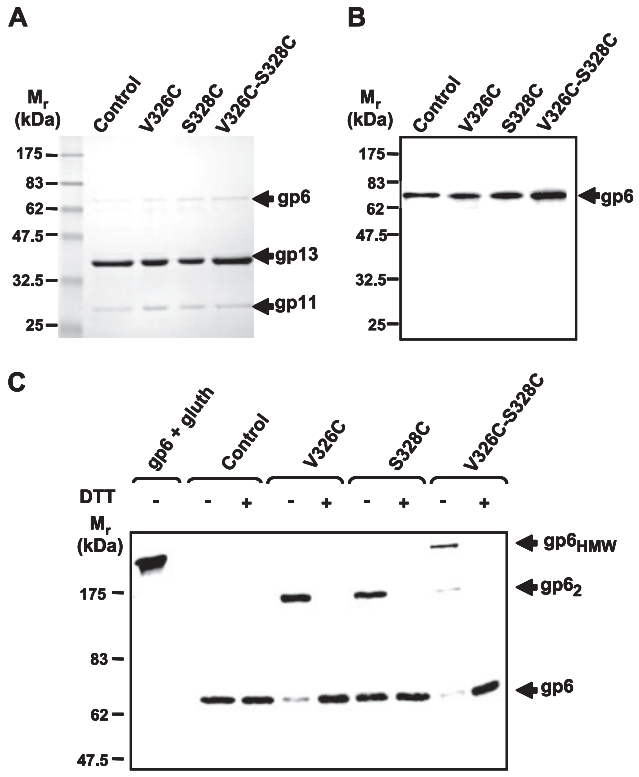

FIGURE 2. **Disulfide bond formation in procapsids carrying control gp6, gp6$_{V326C}$, gp6$_{S328C}$, or gp6$_{V326C/S328C}$.** Shown are SDS-polyacrylamide gels stained with Coomassie Blue (*A*) and a Western blot developed with anti-gp6 of purified SPP1 procapsids carrying the different gp6 forms (*B*). *C*, disulfide bridge formation in gp6 proteins embedded in the procapsid structure. Purified procapsids reduced by the addition of 4 mM DTT (+) or untreated (−) and treated with *N*-ethylmaleimide were resolved in 12% SDS-polyacrylamide gels, and gp6 was detected by Western blotting. gp6 cross-linked with 25 mM glutaraldehyde (*gp6 + gluth*) was used as the control for migration of gp6 oligomers (27). *gp6$_2$*, gp6 dimers; *gp6$_{HMW}$*, high molecular weight gp6.

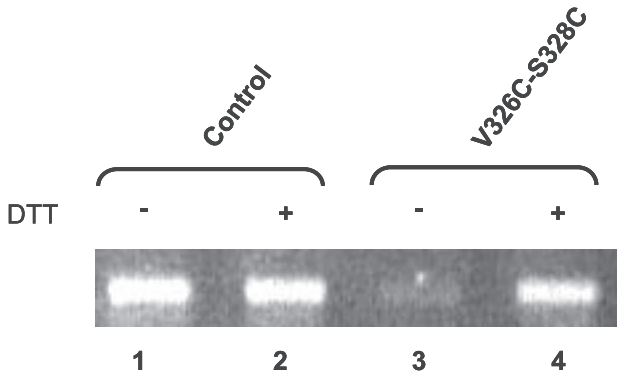

FIGURE 3. **DNA packaging *in vitro* into procapsids carrying gp6c or gp6$_{V326C/S328C}$.** DNA packaging reactions were carried out with purified terminase subunits (gp1 and gp2) and procapsids. Procapsids were preincubated in the presence (+) or in the absence (−) of 2 mM DTT for 1 h at 37 °C. DNA packaging *in vitro* was analyzed by a DNase protection assay (24).

of the gel did not allow us to conclude that these gp6$_{HMW}$ species correspond to covalent bonding of the complete cyclical oligomer through disulfide bridges. However, the lack of a ladder of gp6 forms resulting from a different number of subunits covalently associated, and the strong signal of the high molecular species relative to the single subunit band showed that most of the subunits of the oligomer established disulfide bonds. Note that the intensity of the band corresponding to cross-linked gp6 might, in fact, be an underestimation of this species because of the less efficient transfer of very high molecular weight proteins in the Western blot (688 kDa for the gp6 12-mer). All of the mutants modeled to establish disulfide bridges in the gp6 13-mer (V326C/S328C, V326C/K331C, and V326C/E332C) led to the appearance of gp6$_{HMW}$ (Table 2). Cross-linked gp6 was observed also in the case of D327C/S328C, implying a structural flexibility that allowed the two residues to move ~2 Å toward each other for disulfide bridge formation (Table 1). In contrast, D327C and S328C were appropriately positioned in the gp6 12-mer to make a disulfide bond in the procapsid structure. Mutants V326C/S328C and V326C/E332C also formed disulfide bonds in the 12-mer, whereas V326C/K331C did not (Table 2), as expected from modeling (Table 1). These results validate the quality of the gp6 12-mer pseudoatomic structure and its differences relative to the 13-mer structure.

Impact of Mutations in SPP1 Portal Protein Function—The biological activity of engineered gp6 mutant forms was quantified by complementation assays *in vivo*. The reducing bacterial cytoplasm environment allowed the determination of the effect of the substitutions into cysteine on portal protein function in the absence of disulfide bridge formation. Low complementation values were obtained for the D327C/S328C, V326C/E332C, and V326C/K331C double cysteine gp6 mutants (Table 2), demonstrating that these mutations affect portal protein function *per se*, when no intersubunit cross-linking occurs. Analysis of procapsid protein content revealed that these pairs of amino acid substitutions reduced significantly the incorporation of gp6 in the procapsid (Table 2), as previously found for numerous mutations in residues 329–343 of α5 (16). The double mutant V326C/S328C was active in complementation assays in spite of the fact that single mutants V326C and S328C presented low complementation values *in vivo*. These two neighbor residues did not establish direct contacts. However, their close proximity in the gp6 structure (Fig. 1, *E* and *F*) was compatible with an effect of allele-specific suppression, in which a deleterious mutation in one residue is compensated by a second mutation in a different residue, restoring biological activity. Gp6$_{V326C/S328C}$ was incorporated into wild-type levels in SPP1 procapsids (Fig. 2, *A* and *B*, and Table 2). This mutant was thus suitable to test the effect on DNA packaging of the reversible immobilization of adjacent helices α5 through disulfide bridges.

Immobilization of α5 Helices by Intersubunit Disulfide Bridges Reversibly Blocks DNA Packaging—DNA packaging reactions with purified components (24) were carried out with procapsids containing control gp6 or gp6$_{V326C/S328C}$ preincubated in the presence or in the absence of DTT. Under reducing conditions, the packaging efficiency, assayed by a DNase protection assay, was identical in procapsids carrying control or mutant portals (Fig. 3, *lanes 2* and *4*). In contrast, α5–α5 intersubunit disulfide bond formation (Fig. 2*C*) led to a drastic reduction of DNA packaged through the gp6$_{V326C/S328C}$ portal channel (Fig. 3, *lanes 3* and *4*).

Helix α5–α5 Disulfide Bridge Cross-linking Does Not Impair DNA Traffic through the Portal Tunnel—To demonstrate that movements of helix α5 are necessary for DNA translocation, it

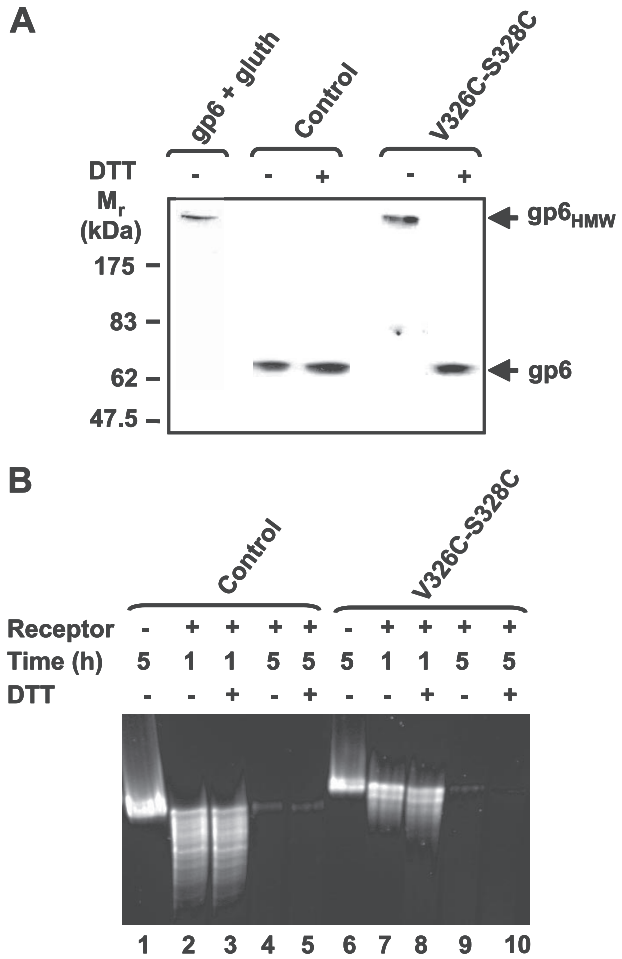

FIGURE 4. **DNA ejection *in vitro* from purified SPP1 virions carrying control gp6 or $gp6_{V326C-S328C}$.** *A*, disulfide bond formation and reduction in CsCl-purified phage particles assayed as in Fig. 2*C*. *B*, DNA ejection from virions incubated with the SPP1 receptor ectodomain (YueB780). Phage particles mixed with nucleases were reduced with 2 mM DTT or left untreated and then incubated with the receptor ectodomain on ice. Samples were shifted to 15 °C to trigger DNA release, and the reaction was stopped after 1 or 5 h, as shown on the *top* of the gel lanes. DNA protected from DNase treatment was resolved by pulsed field gel electrophoresis followed by staining with SybrGold (Molecular Probes).

was important to exclude the possibility that disulfide bridges could lead simply to closure of the portal tunnel, preventing DNA passage. During viral genome ejection, DNA exits the viral capsid through the portal tunnel in a process driven by its tight packing inside the virion (step from states III to IV in Fig. 1*A*). In this case, when disulfide bridges lead to obstruction of the tunnel, DNA exit should be affected. We thus produced phage particles carrying either control gp6 or $gp6_{V326C/S328C}$ to analyze DNA ejection. *B. subtilis* YB886 producing each of the two proteins were infected with SPP1*sus115delX110* that was defective for gp6 production. Note that phages carrying $gp6_{V326C/S328C}$ package DNA during assembly *in vivo*, because disulfide bridges were not formed in the reducing bacterial cytoplasm. Air oxidation of CsCl-purified phage particles led to the formation of intersubunit disulfide bridges in $gp6_{V326C/S328C}$ that were efficiently reduced by DTT (Fig. 4*A*).

DNA ejection from phages was triggered by incubation with the ectodomain of the SPP1 receptor YueB780 (26). Analysis of the DNA protected inside phage capsids by pulsed field gel electrophoresis after 1 h of ejection at 15 °C showed that comparable amounts of DNA were ejected under oxidation and reduction conditions (Fig. 4*B*). The smear observed underneath the intact SPP1 mature DNA molecule revealed trapped partial ejection events as previously observed (25, 26). After 5 h, most of the DNA was ejected from all phage particles. We noticed that virions containing $gp6_{V326C/S328C}$ packaged DNA molecules larger than those found in phages with control gp6 that carried mutation *sizA* (Fig. 4*B*). The double cysteine amino acid substitution thus compensated for the undersizing effect of the *sizA* mutation in the length of packaged DNA molecules. However, this phenotype results from the cysteine mutations *per se* and not from disulfide bridge formation (Fig. 4*B*, compare *lanes 7* with *8* and *9* with *10*). The ensemble of the results shows that formation of the C326–C328 intersubunit disulfide bridge specifically blocks DNA translocation during viral assembly but does not affect passive DNA traffic through the portal tunnel.

The tight belt formed by tunnel loops, potentially further stabilized by helix α5 covalent bonding, could potentially impose a constraint for DNA exit during viral genome ejection. However, we know that the portal by itself cannot avoid the exit of DNA from the capsid after DNA packaging is terminated. This requires binding of proteins gp15 and gp16 (Fig. 1*A*, *blue* and *green ovals*, respectively, in states II to IV) to close the portal channel (18). Our interpretation is that the high pressure built inside the capsid by the DNA tight packing (>50 atmospheres (12)) will be exerted on the loops, physically forcing them downwards to a position that allows DNA passage when the portal channel is open. Note that there was plenty of room to accommodate the loops in the cavity defined underneath each tunnel loop and the tilted helix α5 (Fig. 1*C*). Furthermore, small motions of α5 helices, which can occur synchronously when the helices are covalently bound, can be associated to large motions of tunnel loops (17). Current knowledge, however, does not allow us to define the structural rearrangement in the loops that opens the way for DNA exit. Finally, we note that DNA translocation and ejection from viral capsids are not symmetric mechanisms. The first is an active process of DNA transport that most probably requires sequential motions of helix α5 and tunnel loops for individual translocation steps energized by ATP hydrolysis. In contrast, DNA ejection is a passive process driven by the tight packing of DNA inside the capsid requiring only an open path for continuous DNA flow toward the phage exterior.

Mechanistic Implications—The main finding stemming from our study is that conformational changes between subunits of the portal protein are essential for function of the viral DNA packaging motor. This is the first experimental evidence for a key role in DNA translocation played by structural adjustments inside the portal protein. The conformational change involves the motion of α5 helices relative to each other. These helices, which are tilted relative to the portal tunnel by ~30°, pack side by side in the portal oligomer, defining the conical shape of the internal surface of the tunnel (Fig. 1*C*). Helix α5 stabilizes the conformation of the tunnel loop that protrudes from each individual subunit toward the tunnel interior (Fig. 1*C*) (17). The narrow diameter defined by the tunnel loops in the 12-mer structure implies that their position must change for DNA passage, suggesting a role for movements of helix α5 during DNA translocation. Two types of conformational changes can be

envisaged. First, a concerted conformational change in which the 12 portal subunits move synchronously apart, increasing the width of the tunnel for passage of DNA. However, such movement is likely restrained by constraints imposed by the procapsid structure that surrounds the portal oligomer (6, 7, 29, 30). A second and more conceivable possibility is that independent motions of individual portal subunits allow the tunnel loops to adopt an asymmetric arrangement that fits the helical structure of the DNA molecule. Lebedev *et al.* (17) have proposed that differential positioning of the loops in the form of a wave surrounding the DNA correlates with changes in the relative positions of adjacent α5 helices. Motions of these helices provide a path for signal and/or force transmission between the loops interacting with DNA and the viral ATPase (Fig. 1*C*), coordinating changes in loop position with ATP hydrolysis. Such cross-talk was suggested by characterization of mutations in the loop (E352G) and in helix α5 (T319A) that reduce the terminase ATPase activity (13). However, previous studies provide no proof for an essential role of positional rearrangements of α5 helices, or other portal conformational changes, in viral genome packaging. This piece of evidence is provided here and strongly suggests that communication between the portal protein and the ATPase through movements of the portal helix α5 is a central feature of the DNA translocation mechanism.

Structural similarity between known portal proteins suggests that a common mechanism has been retained during evolution for genome translocation in double-stranded DNA viruses. The viral packaging motor appears to be mechanistically more complex than double-stranded DNA motors found in bacterial translocases, such as SpoIIIE or FtsK (31–33). This is because, in addition to the ATPase, the viral motor also contains the portal protein. The use of a two-component motor by the virus offers the selective advantage that the ATPase only engages DNA translocation when assembled at the portal vertex of the procapsid, remaining inactive when free in the cytoplasm. At present, it is not possible to distinguish whether the viral DNA packaging motor was built on the rotary inchworm mechanism proposed for FtsK (34) and previously hypothesized for the packaging ATPase (35), which is based on sequential conformational changes in single subunits, or if it used a different mechanism as the coordinated wave-like motion, where each ATP hydrolysis step involves a coordinated rearrangement in all subunits of the motor (17, 36). Our current working hypothesis is that sequential firing of the viral ATPase (see also Ref. 3), probably a hexamer, is coordinated with the position of DNA in the tunnel via structural adjustments in α5 helices. We note that, when a tunnel loop enters the DNA major groove, the viral ATPase could be also correctly positioned to interact with the major groove along the same vertical plane, two helix turns apart (Fig. 1*C*). The coordinated sequential action of the ATPase and of tunnel loops on DNA, as proposed also for the α and β domains of FtsK (33), could be critical for continuous engagement of the packaging machinery on the double helix to reach paracrystalline concentrations of nucleic acid inside the viral capsid.

Acknowledgments—We are indebted to Sandrine Brasilès for technical help during DNA ejection experiments.

REFERENCES

1. Valpuesta and Carrascosa (1994) *Q. Rev. Biophys.* **27,** 107–155
2. Tao, Y., Xu, W., Anderson, D. L., Rossmann, M. G., and Baker, T. S. (1998) *Cell* **95,** 431–437
3. Chemla, Y. R., Aathavan, K., Michaelis, J., Grimes, S., Jardine, P. J., Anderson, D. L., and Bustamante, C. (2005) *Cell* **122,** 683–692
4. Carson, M. (1997) *Methods Enzymol.* **277,** 493–505
5. Simpson, A. A., Tao, Y., Leiman, P. G., Badasso, M. O., He, Y., Jardine, P. J., Olson, N. H., Morais, M. C., Grimes, S., Anderson, D. L., Baker, T. S., and Rossmann, M. G. (2000) *Nature* **408,** 745–750
6. Agirrezabala, X., Martin-Benito, J., Caston, J. R., Miranda, R., Valpuesta, J. M., and Carrascosa, J. L. (2005) *EMBO J.* **24,** 3820–3829
7. Jiang, W., Chang, J., Jakana, J., Weigele, P., King, J., and Chiu, W. (2006) *Nature* **439,** 612–616
8. Jardine, P. J., and Anderson, D. L. (2006) in *The Bacteriophages* (Calendar, R., ed) pp. 49–65, Oxford University Press, New York
9. Guo, P., Peterson, C., and Anderson, D. (1987) *J. Mol. Biol.* **197,** 219–228
10. Rao, V. B., and Black, L. W. (1987) *Mol. Biol.* **200,** 475–488
11. Morita, M., Tasaka, M., and Fujisawa, H. (1993) *Virology* **193,** 748–752
12. Catalano, C. E. (2005) in *Viral Genome Packaging Machines: Genetics, Structure, and Mechanism* (Catalano, C. E., ed) pp. 1–4, Kluwer Academic/Plenum Publishers, New York
13. Oliveira, L., Henriques, A. O., and Tavares, P. (2006) *J. Biol. Chem.* **281,** 21914–21923
14. Yeo, A., and Feiss, M. (1995) *J. Mol. Biol.* **245,** 141–150
15. Isidro, A., Henriques, A. O., and Tavares, P. (2004) *Virology* **322,** 253–263
16. Isidro, A., Santos, M. A., Henriques, A. O., and Tavares, P. (2004) *Mol. Microbiol.* **51,** 949–962
17. Lebedev, A. A., Krause, M. H., Isidro, A. L., Vagin, A., Orlova, E. V., Turner, J., Dodson, E. J., Tavares, P., and Antson, A. A. (2007) *EMBO J.* **26,** 1984–1994
18. Orlova, E. V., Gowen, B., Droge, A., Stiege, A., Weise, F., Lurz, R., van Heel, M., and Tavares, P. (2003) *EMBO J.* **22,** 1255–1262
19. Petersen, M. T., Jonson, P. H., and Petersen, S. B. (1999) *Protein Eng.* **12,** 535–548
20. Emsley, P., and Cowtan, K. (2004) *Acta Crystallogr. Sect. D Biol. Crystallogr.* **60,** 2126–2132
21. Tavares, P., Santos, M. A., Lurz, R., Morelli, G., de Lencastre, H., and Trautner, T. A. (1992) *J. Mol. Biol.* **225,** 81–92
22. Chai, S., Bravo, A., Luder, G., Nedlin, A., Trautner, T. A., and Alonso, J. C. (1992) *J. Mol. Biol.* **224,** 87–102
23. Sambrook, J., Maniatis, T., and Fritsch, E. (1989) in *Molecular Cloning, A Laboratory Manual*, 2nd Ed., pp. 1.21–1.45, Cold Spring Harbor Laboratory, Cold Spring Harbor, NY
24. Oliveira, L., Alonso, J. C., and Tavares, P. (2005) *J. Mol. Biol.* **353,** 529–539
25. Vinga, I., Dröge, A., Stiege, A. C., Lurz, R., Santos, M. A., Daugelavicius, R., and Tavares, P. (2006) *Mol. Microbiol.* **61,** 1609–1621
26. São-José, C., Lhuillier, S., Lurz, R., Melki, R., Lepault, J., Santos, M. A., and Tavares, P. (2006) *J. Biol. Chem.* **281,** 11464–11470
27. Jekow, P., Behlke, J., Tichelaar, W., Lurz, R., Regalla, M., Hinrichs, W., and Tavares, P. (1999) *Eur. J. Biochem.* **264,** 724–735
28. Betanzos, M., Chiang, C. S., Guy, H. R., and Sukharev, S. (2002) *Nat. Struct. Biol.* **9,** 704–710
29. Morais, M. C., Choi, K. H., Koti, J. S., Chipman, P. R., Anderson, D. L., and Rossmann, M. G. (2005) *Mol. Cell* **18,** 149–159
30. Tang, L., Marion, W. R., Cingolani, G., Prevelige, P. E., and Johnson, J. E. (2005) *EMBO J.* **24,** 2087–2095
31. Bath, J., Wu, L. J., Errington, J., and Wang, J. C. (2000) *Science* **290,** 995–997
32. Saleh, O. A., Perals, C., Barre, F. X., and Allemand, J. F. (2004) *EMBO J.* **23,** 2430–2439
33. Pease, P. J., Levy, O., Cost, G. J., Gore, J., Ptacin, J. L., Sherratt, D., Bustamante, C., and Cozzarelli, N. R. (2005) *Science* **307,** 586–590
34. Massey, T. H., Mercogliano, C. P., Yates, J., Sherratt, D. J., and Lowe, J. (2006) *Mol. Cell* **23,** 457–469
35. Camacho, A. G., Gual, A., Lurz, R., Tavares, P., and Alonso, J. C. (2003) *J. Biol. Chem.* **278,** 23251–23259
36. Enemark, E. J., and Joshua-Tor, L. (2006) *Nature* **442,** 270–275

Structural Rearrangements between Portal Protein Subunits Are Essential for Viral DNA Translocation

Ana Cuervo, Marie-Christine Vaney, Alfred A. Antson, Paulo Tavares and Leonor Oliveira

J. Biol. Chem. 2007, 282:18907-18913.
doi: 10.1074/jbc.M701808200 originally published online April 18, 2007
